Monthly Notices
of the
ROYAL ASTRONOMICAL SOCIETY

MNRAS **428,** 1950–1957 (2013) doi:10.1093/mnras/sts147

Why do stars form in clusters? An analytic model for stellar correlation functions

Philip F. Hopkins★

Department of Astronomy, University of California Berkeley, Berkeley, CA 94720, USA

Accepted 2012 October 4. Received 2012 October 4; in original form 2012 February 9

ABSTRACT

Recently, we have shown that if the interstellar medium is governed by supersonic turbulent flows, the excursion-set formalism can be used to calculate the statistics of self-gravitating objects over a wide range of scales. On the largest self-gravitating scales ('first crossing'), these correspond to giant molecular clouds (GMCs), and on the smallest non-fragmenting self-gravitating scales ('last crossing'), to protostellar cores. Here, we extend this formalism to rigorously calculate the autocorrelation and cross-correlation functions of cores (and by extension, young stars) as a function of spatial separation and mass, in analogy to the cosmological calculation of halo clustering. We show that this generically predicts that star formation is very strongly clustered on small scales: stars form in clustered regions, themselves inside GMCs. Outside the binary-star regime, the projected correlation function declines as a weak power law, until a characteristic scale which corresponds to the characteristic mass scale of GMCs. On much larger scales the clustering declines such that star formation is not strongly biased on galactic scales, relative to the actual dense gas distribution. The precise correlation function shape depends on properties of the turbulent spectrum, but its qualitative behaviour is quite general. The predictions agree well with observations of young star and core autocorrelation functions over $\sim$4 dex in radius. Clustered star formation is a generic consequence of supersonic turbulence if most of the power in the velocity field, hence the contribution to density fluctuations, comes from large scales $\sim h$. The distribution of self-gravitating masses near the sonic length is then imprinted by fluctuations on larger scales. We similarly show that the fraction of stars formed in 'isolated' modes should be small, $\lesssim$10 per cent.

Key words: galaxies: active – galaxies: evolution – galaxies: formation – galaxies: star formation – cosmology: theory.

1 INTRODUCTION

A central tenet of our understanding of star formation is that star formation is clustered or correlated (e.g. Lada & Lada 2003; Portegies Zwart, McMillan & Gieles 2010 and references therein). Observational evidence for this comes from a number of channels: observations have directly measured the correlation between young O-stars and other populations (Oey, King & Parker 2004; Parker & Goodwin 2007), and shown that most can be directly identified as part of young clusters/associations (Gies 1987), with most of the remainder being identifiable as runaways (de Wit et al. 2005; Schilbach & Röser 2008). The observed star formation rate (SFR) in embedded clusters in the Milky Way (MW) can account for most of the large-scale average SFR (Lada & Lada 2003). The correlation function of stars in various MW star-forming regions has been measured and rises continuously on small scales, over >4–5 orders of magnitude in radius (Gomez et al. 1993; Larson 1994; Simon 1997; Nakajima et al. 1998; Clarke, Bonnell & Hillenbrand 2000; Hartmann 2002; Hennekemper et al. 2008; Kraus & Hillenbrand 2008). In nearby galaxies the observations are more difficult, but in starburst galaxies a large fraction of all the ultraviolet light is often identified with just a few young star clusters, themselves clustered (see e.g. Zhang, Fall & Whitmore 2001 and references therein).

Theoretically, this is broadly understood as a consequence of dense gas being concentrated primarily in GMCs, which then undergo fragmentation and turn some fraction of their mass into stars. And it does appear that the same clustering is evident in the prestellar/protostellar core population (Stanke et al. 2006). However, this does not provide a quantitative model for their correlation function, nor does it actually explain why this should be the case – why do most stars not form in relatively more isolated high-density regions?

★ E-mail: phopkins@astro.berkeley.edu

Although much theoretical progress has been made in understanding how stars form in clusters, our fundamental understanding of why their formation is clustered remains quite limited. There is no analytic theory for the star–star correlation function, outside of very small scales where it is dominated by the binary-star population. Much of the discussion in the literature has focused on determining the fractal dimension of star formation: if the interstellar medium (ISM) were structured in a hierarchically fractal manner, this would imply a simple power-law correlation function from which the fractal dimension can be determined. Moreover, this is not a physical, predictive model; it is a parametrization – albeit a useful one – of the observations (see also Bate, Clarke & McCaughrean 1998). Moreover, it must break down at both small scales (the binary regime) and large scales, since it is also observationally established that star formation is not strongly clustered/biased relative to the dense gas in the disc on very large scales (Zhang et al. 2001; Leroy et al. 2008; Foyle et al. 2010).

At first glance, it is not surprising that there is no more sophisticated analytic theory for the correlation function of stars. The process is highly non-linear, chaotic and involves a wide range of physics including turbulence, cooling, magnetic fields and feedback, and the correlation function is a spatially dependent quantity. There have therefore been some attempts to compare stellar correlation functions with numerical simulations of star formation in clusters (see Klessen & Burkert 2000; Hansen et al. 2012), but the dynamic range of the problem makes this very difficult. Galaxy-scale simulations are required to follow the formation of GMCs and predict their global properties, and how these overdense regions compare to the density field in more isolated regions (i.e. why there are not more stars in non-clustered regions). Moreover, these cannot resolve the formation of stars and model it with subgrid recipes – the typical 'star particle' in such simulations is the mass of a real star cluster. Simulations which have the necessary resolution can only follow small 'protocluster' regions whose properties must be assumed as initial conditions; they can predict quantities such as the binary distribution, but not global clustering.

However, Hopkins (2012a, hereafter Paper I) recently generalized the excursion-set formalism – well known from cosmological applications as a means to calculate halo mass functions and clustering – to calculate the statistics of bound objects in the density field of the turbulent ISM. The key property of supersonic turbulence that makes this possible is that the density distribution (at least outside of collapsed regions) tends towards a lognormal, with a dispersion that varies in a well-defined manner with Mach number (see e.g. Vazquez-Semadeni 1994; Padoan, Nordlund & Jones 1997; Ostriker, Gammie & Stone 1999). In Paper I, we use this to construct the statistics of the 'first-crossing distribution': the statistics of bound objects defined on the largest scales on which they are self-gravitating. We showed that the predicted mass function and correlation functions/clustering properties agree well with observations of GMCs on galactic scales. In Hopkins (2012b, hereafter Paper II), we extended the formalism to the 'last-crossing distribution' – specifically, the mass function of bound objects defined on the smallest scales on which they remain self-gravitating but do not have self-gravitating subregions (i.e. are not fragmenting). We argued that these should be associated with protostellar cores, and in Paper II showed that the resulting core mass function (MF) agrees well with canonical MW core mass function (CMF) and (by extrapolation) stellar initial mass functions (IMFs). This formalized the approximate argument for the same in Hennebelle & Chabrier (2008), but more importantly for our purposes here, places it in the proper excursion-set formalism and so makes it possible to calculate higher order statistics such as clustering properties, using only information on global (galactic) scales.

In this paper, we use the excursion-set formalism, in analogy to its well-studied application for the clustering of dark matter haloes, to develop a fully analytic theory for the clustering of protostellar cores and, by extension, star formation, in a turbulent ISM.

Before going forward, we must make a critical distinction between 'clustered' star formation and star formation 'in (bound) clusters'. Whether or not a population is 'clustered' is a general statement about whether it follows a non-zero two-point correlation function (i.e. if members of the population are more likely to appear near other members of the population, relative to their spatial distribution if the objects were randomly distributed in the volume). This is the sense we will refer to throughout the paper, for which we can calculate the correlation function and clustering amplitude, for any scale on which the clustering is evaluated. Whether stars are 'in clusters' depends on the definition of 'a cluster', which is not generic; long-lived clusters must be gravitationally bound, which requires consideration of quantities like the mass expelled as stars form and evolve (not included in our study here). This is a very different question, and is outside the scope of this paper (see e.g. Bressert et al. 2010 and references therein).

In Section 2 we derive the solution for the statistics of the last-crossing distribution inside a large-scale overdensity/underdensity (the mathematical underpinning of the correlation function). In Section 3 we show how this relates to the conditional mass function of cores. In Section 4 we use this to derive the star–star correlation functions. In Section 5 we present the calculated correlation functions as a function of stellar mass and spatial scale, as well as global turbulent ISM properties, and compare to observations. In Section 6 we summarize our results and discuss their implications.

2 THE TWO-BARRIER LAST-CROSSING PROBLEM

Calculating clustering properties in the excursion-set formalism depends on the solution to the 'two-barrier problem' – the probability of an 'event' given a specific value of the Gaussian field at some larger scale. This is well studied for the first-crossing events, but has not been calculated for the last-crossing distribution; we therefore calculate this here. Our derivation closely follows that in Paper II.

Consider the Gaussian field $\delta(\boldsymbol{x} \mid R)$ (which here represents the logarithmic density field smoothed in a kernel of radius R about $\boldsymbol{x}$). The variance $S(R)$ is monotonic so we take S as the independent variable and consider $\delta(S)$ (for convenience, we will drop explicit notation of $\boldsymbol{x}$). The probability distribution function of $\delta(S)$ is, by definition,

$$P_0(\delta \mid S) = \frac{1}{\sqrt{2\pi\, S}}\, \exp\left(-\frac{\delta^2}{2\, S}\right). \quad (1)$$

The barrier $B(S)$ is the minimum value $\delta(S)$ which defines objects of interest (e.g. collapsing regions). Consider a 'trajectory' $\delta(S)$ which begins at some δ_i at $S_i(R_i \rightarrow 0)$, then evaluate it at successively larger scales (smaller S). We define last-crossing distribution in Paper II, $f_\ell(S \mid \delta_i)\, \mathrm{d}S$, as the probability that the trajectory crosses $B(S)$ for the first time between S and $S + \mathrm{d}S$ *without* having crossed $B(S)$ at any larger S. The sum over all trajectories is just given by $f_\ell(S) \equiv \int f_\ell(S \mid \delta_i)\, P(\delta_i)\, \mathrm{d}\delta_i$.

Define $f_\ell(S \mid \delta_0)$ as the value of $f_\ell(S)$, for trajectories which have a value $\delta(S_0) = \delta_0$ at some *larger* scale S_0. Moreover, define $\Pi(\delta[S] \mid \delta_0[S_0])\, \mathrm{d}\delta$ as the probability for a trajectory – constrained to have $\delta_0(S_0)$ – to have a value between δ and $\delta + \mathrm{d}\delta$ at scale S,

without having crossed $B(S)$ at any larger $S' > S$. The integrals of $f_\ell(S \,|\, \delta_0)$ and $\Pi(\delta[S] \,|\, \delta_0[S_0])$ for $\delta < B(S)$ must sum to unity:

$$1 = \int_S^{S_i} \mathrm{d}S'\, f_\ell(S' \,|\, \delta_0) + \int_{-\infty}^{B(S)} \Pi(\delta[S] \,|\, \delta_0[S_0])\, \mathrm{d}\delta. \quad (2)$$

If we ignored the barrier, $\Pi(\delta[S] \,|\, \delta_0[S_0])$ would be equal to $P_{10}(\delta[S] \,|\, \delta_0[S_0])$, the probability that a trajectory with $\delta_0(S_0)$ has a value $\delta(S)$ at a larger $S > S_0$. This is just

$$P_{10}(\delta[S] \,|\, \delta_0[S_0]) = P_0(\delta - \delta_0 \,|\, S - S_0). \quad (3)$$

Moreover, we must subtract from this the probability that a trajectory crosses the barrier at some larger $S' > S$ and then passes through $\delta(S)$, so

$$\begin{aligned}\Pi(\delta[S] \,|\, \delta_0[S_0]) &= P_{10}(\delta[S] \,|\, \delta_0[S_0]) \\ &\quad - \int_S^{S_i} \mathrm{d}S'\, f_\ell(S' \,|\, \delta_0)\, P_{01}(\delta[S] \,|\, \delta' \\ &= B[S',\ \delta_0[S_0]), \end{aligned} \quad (4)$$

where $P_{01}(\delta[S] \,|\, \delta'[S'], \delta_0[S_0])$ is the probability of a transition from $\delta(S')$ to $\delta(S)$ where $S' > S$ – i.e. moving in the 'opposite' direction (decreasing S) from the transition which defined P_{10} – for a trajectory subject to the constraint that it must equal δ_0 at S_0. This can be determined from Bayes' theorem:

$$P_{01}(\delta[S] \,|\, B[S']) = P_{10}(B[S'] \,|\, \delta[S])\, \frac{P_{10}(\delta[S] \,|\, \delta_0[S_0])}{P_{10}(B[S'] \,|\, \delta_0[S_0])}, \quad (5)$$

where on the right-hand side we have $P_{10}(\delta[S] \,|\, \delta_0[S_0])$ and $P_{10}(B[S'] \,|\, \delta_0[S_0])$ instead of $P_0(\delta \,|\, S)$ and $P_0(B[S'] \,|\, S')$ because the distributions are constrained to have $\delta_0(S_0)$. Moreover, because fluctuations on successive scales are uncorrelated, the probability $P_{10}(B[S'] \,|\, \delta[S])$ does not explicitly depend on δ_0.

The governing equation for $f_\ell(S \,|\, \delta_0)$ is now completely defined in terms of normal distributions. We can therefore follow exactly the procedure in Paper II. After differentiating equation (2) to isolate $f_\ell(S \,|\, \delta_0)$ and performing a considerable amount of simplifying integral evaluation,[1] we arrive at the key equation for $f_\ell(S \,|\, \delta_0)$:

$$f_\ell(S \,|\, \delta_0) = g_1(S \,|\, \delta_0) + \int_S^{S_i} \mathrm{d}S'\, f_\ell(S' \,|\, \delta_0)\, g_2(S,\ S' \,|\, \delta_0), \quad (6)$$

where

$$g_1(S \,|\, \delta_0) = \left[2\,\frac{\mathrm{d}B}{\mathrm{d}S} - \frac{B(S) - \delta_0}{S - S_0}\right] P_0(B(S) - \delta_0 \,|\, S - S_0), \quad (7)$$

$$\begin{aligned} g_2(S,\ S' \,|\, \delta_0) = &\left[\frac{B(S') - B(S)}{S' - S} + \frac{B(S) - \delta_0}{S - S_0} - 2\,\frac{\mathrm{d}B}{\mathrm{d}S}\right] \\ &\times P_0[B(S) - \delta_e(S,\ S') \,|\, S_e(S,\ S')], \end{aligned} \quad (8)$$

$$\delta_e(S,\ S') = B(S') + (\delta_0 - B[S'])\left(\frac{S' - S}{S' - S_0}\right), \quad (9)$$

$$S_e(S,\ S') = (S' - S)\left(\frac{S - S_0}{S' - S_0}\right). \quad (10)$$

Although complicated, equation (6) has, in general, a unique solution for any arbitrary barrier $B(S)$, and is straightforward to solve via standard numerical methods for any choice $\delta_0(S_0)$ provided $S_0 < S$ (see the discussion in Paper II and Zhang & Hui 2006).

In fact for a linear barrier, $B(S) = B_0 + \beta\, S$; this has a remarkably simple closed-form solution:

$$f_\ell(S \,|\, \delta_0)|_{B = B_0 + \beta\, S} = \beta\, P_0(B[S - S_0] - \delta_0 \,|\, S - S_0). \quad (11)$$

It is easy to verify that when $\delta_0 \to 0$ as $S_0 \to 0$, we recover the one-barrier last-crossing distribution from Paper II, which is the value of $f_\ell(M \,|\, \delta_0)$ averaged over all $\delta_0(S_0)$:

$$f_\ell(M) \equiv \langle f_\ell(M \,|\, \delta_0) \rangle = f_\ell(M \,|\, \delta_0 \to 0,\ S_0 \to 0). \quad (12)$$

3 THE CONDITIONAL MASS FUNCTION

In Paper I, we derive $S(R)$ and $B(S)$ from simple theoretical considerations for all scales in a galactic disc. For a given turbulent power spectrum, with the assumption that the disc is marginally stable (Toomre $Q = 1$), $S(R)$ is determined by summing the contribution from the velocity variance on all scales $R' > R$

$$S(R) = \int_0^\infty |W(k,\ R)|^2 \ln\left[1 + \frac{3}{4}\,\frac{v_\mathrm{t}^2(k)}{c_\mathrm{s}^2 + \kappa^2\, k^{-2}}\right] \mathrm{d}\ln k, \quad (13)$$

where W is the window for the density smoothing,[2] $v_\mathrm{t}(k)$ is the turbulent velocity dispersion averaged on a scale k (trivially related to the turbulent power spectrum), c_s is the thermal sound speed and κ is the epicyclic frequency ($=\sqrt{2}\,\Omega$, where $\Omega = V_\mathrm{c}/R$ is the orbital frequency for a disc with constant circular velocity V_c). The equation for $B(R)$ is as follows:

$$B(R) = \ln\left(\frac{\rho_\mathrm{crit}}{\rho_0}\right) + \frac{S(R)}{2}, \quad (14)$$

where ρ_crit is the critical density above which a region is self-gravitating. This is

$$\frac{\rho_\mathrm{crit}}{\rho_0} \equiv \frac{1}{2\,\tilde{\kappa}}\left(1 + \frac{h}{R}\right)\left[\frac{\sigma_\mathrm{g}^2(R)}{\sigma_\mathrm{g}^2(h)}\,\frac{h}{R} + \tilde{\kappa}^2\,\frac{R}{h}\right], \quad (15)$$

where ρ_0 is the mean mid-plane density of the disc, h is the disc scale height, $\tilde{\kappa} = \kappa/\Omega = \sqrt{2}$ for a constant-V_c disc and

$$\sigma_\mathrm{g}^2(R) = c_\mathrm{s}^2 + v_\mathrm{A}^2 + \langle v_\mathrm{t}^2(R) \rangle \quad (16)$$

[1] Taking $\mathrm{d}/\mathrm{d}S$ of equation (2), we obtain

$$f_\ell(S|\delta_0) = \frac{\mathrm{d}B}{\mathrm{d}S}\,\Pi(B[S]|\delta_0[S_0]) + \int_{-\infty}^{B(S)} \mathrm{d}\delta\,\frac{\mathrm{d}}{\mathrm{d}S}\,\Pi(\delta[S]|\delta[S_0]).$$

Noting $S' > S > S_0$, equation (5) can be simplified to

$$P_{01}(\delta[S] \,|\, B[S']) = P_0(\delta[S] - \delta_e[S,\ S'] \,|\, S_e[S,\ S']),$$

where δ_e and S_e are defined in equations (9) and (10). We then expand Π using equation (4), take the derivatives with respect to S where appropriate and use the simplifying relations

$$\int_{-\infty}^{B[S]} \mathrm{d}\delta\,\frac{\mathrm{d}}{\mathrm{d}S}\,P_0(\delta - \delta_0|S - S_0) = -\frac{B[S] - \delta_0}{2\,(S - S_0)}\,P_0(B[S] - \delta_0|S - S_0),$$

$$\mathrm{Limit}\left[\int_{-\infty}^{B[S]} \mathrm{d}\delta\, P_{01}(\delta[S] \,|\, B[S'])\right]_{S' \to S} = \frac{1}{2},$$

$$\int_{-\infty}^{B[S]} \mathrm{d}\delta\,\frac{\mathrm{d}}{\mathrm{d}S}\,P_{01}(\delta[S] \,|\, B[S'])$$

$$= -\frac{1}{2}\left[\frac{B(S') - B(S)}{S' - S} + \frac{B(S) - \delta_0}{S - S_0}\right] P_0(B[S] - \delta_e[S,\ S'] \,|\, S_e[S,\ S']).$$

[2] For convenience we take this to be a k-space tophat inside $k < 1/R$, which is implicit in our previous derivation, but we show in Papers I and II that this has little effect on our results.

(v_A is the Alfvén speed). The mapping between radius and mass is

$$M(R) \equiv 4\,\pi\,\rho_{\rm crit}\,h^3\left[\frac{R^2}{2\,h^2}+\left(1+\frac{R}{h}\right)\,\exp\left(-\frac{R}{h}\right)-1\right]. \quad (17)$$

It is easy to see that on small scales, these scalings reduce to the Jeans criterion for a combination of thermal (c_s), turbulent (v_t) and magnetic (v_A) support, with $M = (4\pi/3)\,\rho_{\rm crit}\,R^3$; on large scales, it becomes the Toomre criterion with $M = \pi\Sigma_{\rm crit}\,R^2$.

Recall $f_\ell(S)\,{\rm d}S$ gives the differential fraction trajectories that have a last crossing in a narrow range dS about the scale $S[R]$ (corresponding to mass $M = M[R]$). Each trajectory randomly samples the Eulerian volume, so the differential number of last-crossing regions is related by $V_{\rm cl}(M)\,{\rm d}N(M) = V_{\rm tot} f_\ell(S[M])\,{\rm d}S$ [where $V_{\rm cl}(M) = M/\rho_{\rm crit}(M)$ is the cloud volume at the time of last crossing and $V_{\rm tot}$ is the total volume sampled]. Hence, the mass function – the number density ${\rm d}n = {\rm d}N/V_{\rm tot}$ in a differential interval – is given by

$$\frac{{\rm d}n}{{\rm d}M} = \frac{\rho_{\rm crit}(M)}{M}\,f_\ell(M)\left|\frac{{\rm d}S}{{\rm d}M}\right|. \quad (18)$$

Two parameters completely specify the model in dimensionless units. These are the spectral index p of the turbulent velocity spectrum, $E(k) \propto k^{-p}$ (usually $p \approx 5/3$–2), and its normalization, which we define by the Mach number on large scales $\mathcal{M}_h^2 \equiv \langle v_t^2(h)\rangle/(c_s^2 + v_A^2)$. The dimensional parameters h (or c_s) and ρ_0 simply rescale the predictions to absolute units.

For a choice of p and $\mathcal{M}_h$, it is straightforward to numerically determine $f_\ell(M\,|\,\delta_0[R_0])$, hence the conditional mass function (mass function within the appropriate subregions for any choice of δ_0 and R_0). Unfortunately a closed-form solution is not generally possible. However, we show in Paper II that on sufficiently small scales [near/below the sonic length $R_{\rm sonic} = h\,\mathcal{M}_h^{-2/(p-1)}$], the 'run' in $S(R) \approx S(R_{\rm sonic})$ becomes small (since most of the power contributing in equation 13 comes from large scales), while $B(R)$ rises rapidly, so ${\rm d}B/{\rm d}S \gg B(S)/S \gg 1$. In this limit, the conditional MF is approximately

$$\frac{{\rm d}n}{{\rm d}M} \sim \frac{\rho_{\rm crit}(M)}{M^2}\left|\frac{{\rm d}\ln\rho_{\rm crit}}{{\rm d}\ln M}\right| P_0(\delta-\delta_0\,|\,S-S_0), \quad (19)$$

where

$$P_0(\delta-\delta_0\,|\,S-S_0) = \frac{1}{\sqrt{2\pi(S-S_0)}} \times \exp\left[-\frac{(\ln[\rho_{\rm crit}/\rho(S_0)]+(S-S_0)/2)^2}{2\,(S-S_0)}\right]. \quad (20)$$

For the appropriate choice of δ_0 on scale R_0, this is the resulting core MF (and so relates to the resulting stellar IMF and SFR) in overdense regions (e.g. GMCs) or 'voids' (inter-GMC gas). Taking $\delta_0 \to 0$ and $R_0 \to \infty$, we recover the galaxy-averaged CMF. In a companion paper (Hopkins 2012c), we consider in detail what this means for how the CMF (and by extension IMF) vary with environmental properties. For our purposes here, though, since we average over a range of masses, this has no effect on our results (and the predicted variation within a galaxy is very weak).

4 THE CORRELATION FUNCTION

The autocorrelation function ξ of a given population is defined as the excess probability of finding another member of the population within a differential volume at a radius r from one such member, i.e.

$$1+\xi_{\rm MM}(r\,|\,M) \equiv \frac{\langle N(r\,|\,M)\rangle}{\langle n(M)\rangle\,{\rm d}V}, \quad (21)$$

where $n(M) = {\rm d}n/{\rm d}M$ at mass M and $N(r\,|\,M)$ is the differential number of objects in the mass range $M, M+{\rm d}M$ found at a radius r from another object with mass M. Moreover, since $n(r\,|\,M) \propto f_\ell(M\,|\,\delta_0[S_0(r)])$, for a region with an overdensity δ_0 on a scale S_0 (corresponding to r), this is just

$$1+\xi_{\rm MM}(r\,|\,M) = \int_{\delta_0}\left(\frac{f_\ell(M\,|\,\delta_0)}{f_\ell(M)}\right) P_*(\delta_0\,|\,S_0[r])\,{\rm d}\delta_0. \quad (22)$$

Here, $P_*(\delta_0\,|\,S_0[r])$ is the probability of $\delta(S_0)$ having the value δ_0 on the scale S_0, *given* that $\delta(S[M]) = B(S[M])$ – i.e. there is a barrier crossing (a core/star) at the 'starting point'. Moreover, the probability of having a last-crossing event at scale $S > S_0$, given a density $\delta_0(S_0)$, is just $f_\ell(M\,|\,\delta_0)$. Therefore, conversely, the probability of $\delta_0(S_0)$ given that crossing is just related by Bayes' theorem is

$$P_*(\delta_0\,|\,S_0[r]) = f_\ell(M\,|\,\delta_0)\,\frac{P_0(\delta_0\,|\,S_0)}{f_\ell(M)}. \quad (23)$$

Therefore, we obtain

$$1+\xi_{\rm MM}(r\,|\,M) = \int_{-\infty}^{\infty}\left(\frac{f_\ell(M\,|\,\delta_0)}{f_\ell(M)}\right)^2 P_0(\delta_0\,|\,S_0[r])\,{\rm d}\delta_0. \quad (24)$$

More accurately, what is typically measured is the star–star or clump–clump correlation function over a broad mass range. We therefore require the cross-correlation between an initial crossing at M_1 and second crossing at some M_2. The logic is identical, however. We then integrate over the appropriate range of M_2 and, finally, average over M_1 (weighted by number density). We obtain

$$1+\xi(r) = \frac{\int {\rm d}W_{M_1}\int {\rm d}W_{M_2}\int_{-\infty}^{\infty} f_\ell(M_1\,|\,\delta_0)\,f_\ell(M_2\,|\,\delta_0)\,P(\delta_0\,|\,S_0)\,{\rm d}\delta_0}{\left(\int {\rm d}W_M\,f_\ell(M)\right)^2}, \quad (25)$$

where

$${\rm d}W_M \equiv \frac{\rho_{\rm crit}(M)}{M}\left|\frac{{\rm d}S(M)}{{\rm d}M}\right|{\rm d}M \quad (26)$$

and the integrals over mass M should be over the appropriate observed core/stellar mass range.

Finally, note that what is generally measured is the projected correlation function $\xi_{\rm 2d}(R_p)$. Projecting $\xi(r)$ is straightforward:

$$\xi_{\rm 2d}(R_p) = \frac{\int_{-\infty}^{\infty} n_0(z)\,\xi_{\rm 3d}\left(\sqrt{R_p^2+z^2}\right)\,{\rm d}z}{\int_{-\infty}^{\infty} n_0(z)\,{\rm d}z}, \quad (27)$$

where z is the line-of-sight direction and $n_0(z)$ is the average abundance expected. Technically this will depend on projection angles (especially in the complicated case of systems inside the MW), but for almost any profile where $n_0 \approx n(M)$ is a weak function of z and then falls off at scales $\gtrsim h$ the results are nearly identical.

5 RESULTS

In Fig. 1, we plot the exact (3d) autocorrelation function from equation (24) as a function of r and M. Recall that in dimensionless units the problem is completely specified by a choice of p and $\mathcal{M}_h$, for which we adopt canonical values $p = 2$ (Burgers turbulence,

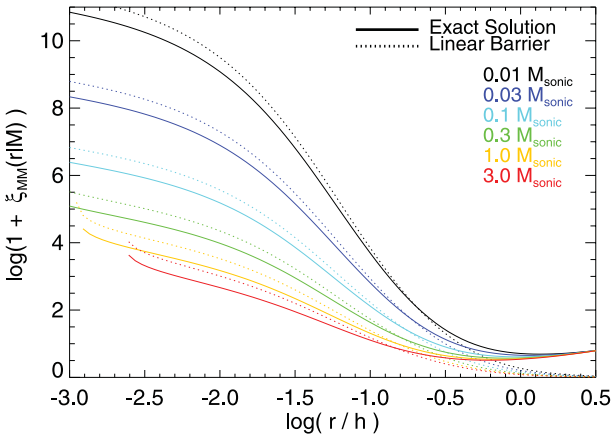

Figure 1. The predicted three-dimensional autocorrelation function of collapsing cores, as a function of radius (in units of the disc scale height h). The excursion-set model for collapsing cores is determined by solving the two-barrier problem for bound/collapsing objects defined at 'last crossing' – i.e. the smallest scales on which they are self-gravitating. The model is completely specified for a given turbulent spectral index p and normalization (which we take to be the Mach number at the scale h, $\mathcal{M}_h$). Here we take $p = 2$, $\mathcal{M}_h = 10$. Solid lines show the exact solution from equation (24). Dotted lines compare the approximate scaling in equation (28) – the normalization is systematically too large, but the shape is correct up to scales $\sim h$, where the assumption that the run in $S(R)$ is small breaks down. The shape is similar at all stellar masses, but the small-scale amplitude increases strongly at low masses. In all cases, cores/stars are predicted to cluster very strongly on small scales, below their parent GMC scale. On large scales ($\gtrsim h$), they are only weakly clustered. The characteristic scale is set by the fact that most of the turbulent velocity power (hence power in density fluctuations) is at this scale.

typical in the supersonic regime) and $\mathcal{M}_h = 10$ (typical of the cold clumps in the MW disc).

The exact results in Fig. 1 require the numerical solution for $f_\ell(M\,|\,\delta_0)$. However, if we restrict to the regime where $\mathrm{d}B/\mathrm{d}S \gg B/S \gg 1$ so that the mass function can be approximated by equation (19), or consider a linear barrier (equation 11), then this has the closed-form solution

$$1 + \xi_{\rm MM}(r\,|\,M) \approx \frac{1}{\sqrt{1-(S_0/S)^2}}\,\exp\left(\frac{B^2}{S\,(1+S/S_0)}\right). \quad (28)$$

At small and large r, respectively, this becomes

$$\xi_{\rm MM}(r\,|\,M) \rightarrow \frac{\exp\,(B^2/2S)}{\sqrt{2\,(1-S_0/S)}} \quad (S_0 \rightarrow S), \quad (29)$$

$$\xi_{\rm MM}(r\,|\,M) \rightarrow \left(\frac{B}{S}\right)^2 S_0 \quad (S_0 \rightarrow 0). \quad (30)$$

We compare this to the exact result. The shape of $\xi(R)$ and its systematic dependence on R are qualitatively described. However, it is nowhere exact because $S(R)$ does vary significantly on larger scales, and $B(R)$ and $S(R)$ both vary such that even if $\mathrm{d}B/\mathrm{d}S \gg 1$, $\mathrm{d}B/\mathrm{d}S \gg B/S$ is less true.

The shape of $\xi_{\rm MM}(r)$ is similar in all cases – i.e. it is nearly mass-independent over the interesting range – so even though the expression for the CMF-averaged cross-correlation $\xi(r)$ in equation (25) is complicated, it mostly amounts to an MF-weighted normalization. What we care about is the correlation function shape (we note below that the observed normalization is arbitrary and should be factored out in any case). This means that regardless of the CMF shape used to 'average' the prediction, the result is similar. For the same reason, provided the general assumption that stars form from self-gravitating cores is reasonable, there will be no large differences between the predicted stellar and core correlation functions, regardless of how this process occurs. If the conversion from core mass to stellar mass were constant, the correlation functions would be exactly identical; but even allowing for a large random variation in conversion efficiency or systematic mass dependence makes little or no difference to our conclusions. We have, for example, considered sampling equation (25) over only different subranges in mass (say sampling only massive stars), or sampling over the full stellar IMF but with a random 0.5 dex scatter in the assumed stellar-to-core mass ratio, or allowing for the stellar-to-core mass ratio to depend on mass $\propto M^{-1}$; in all cases, the differences in the predicted $\xi(r)$ shape are smaller than the differences owing to different choices of the turbulent spectrum. What will change the clustering, on very small scales $\ll R_{\rm sonic}$, is if individual single Jeans-mass cores form multiple stars. And to some extent, this must happen, as many stars are in binary systems. This is not accounted for here; therefore, the predictions cannot be reliably extended to scales below the characteristic core scale $\lesssim R_{\rm sonic}$ (and indeed we see a discrepancy appear at these scales). We discuss this further below.

In analogy to the clustering of dark matter haloes and GMCs defined in Paper I, we can define the linear bias as the ratio of the autocorrelation to the autocorrelation function of the mass itself. On large scales, this should approach a constant:

$$b(M)^2 \equiv \xi/\xi_{\rm mass} \quad (r \rightarrow \infty). \quad (31)$$

On large scales (where $S_0[r]$ is small), the autocorrelation of the mass is just the variance $\xi_{\rm mass} \approx S_0$ (see Mo & White 1996). From equation (30), we can therefore immediately obtain the bias in the limit $\mathrm{d}B/\mathrm{d}S \gg B/S \gg 1$,

$$b(M) \approx \frac{B(S)}{S} \sim 1 - \begin{cases} 0.04\,\ln\,(M/M_{\rm sonic}) & M \gtrsim M_{\rm sonic} \\ 0.17\,\ln\,(M/M_{\rm sonic}) & M \lesssim M_{\rm sonic}, \end{cases} \quad (32)$$

where the latter equality is for typical parameters ($p = 2$, $\mathcal{M}_h \approx 30$) and $M_{\rm sonic} = M(R_{\rm sonic})$. The large-scale bias is a very weak function of mass and is about unity.

In Fig. 2 we plot the projected $\xi_{\rm 2d}$ from equation (27), for the full CMF/IMF-averaged $\xi(r)$.[3] We examine the effects of the two free model parameters: the large-scale Mach number $\mathcal{M}_h$ and turbulent spectral index p. As shown in Paper II for the CMF/IMF, changing $p = 5/3$ instead is nearly equivalent to assuming a higher $\mathcal{M}_h$ at $p = 2$ (since, in both cases, the sonic length is pushed down and turnover at low masses is slower). At lower $\mathcal{M}_h$, decreasing $\mathcal{M}_h$ increases the clustering signal, because there is a smaller variance S, so the small-scale cores depend more heavily on large-scale fluctuations. At sufficiently large $\mathcal{M}_h$, however, there is a significant change in shape in $\xi_{\rm 2d}$; the initial rise below $\sim h$ is rapid, but near $R_{\rm sonic}$, $\xi_{\rm 2d}$ flattens. This is a projection effect: the rise in $\xi_{\rm 3d}$ on small scales is still similar (just slightly more shallow) to that we see in $\xi_{\rm 2d}$ at smaller $\mathcal{M}_h$; however, there is much more power on intermediate scales as well, so the power in $\xi_{\rm 2d}$ is nearly 'converged', hence the flattening.

[3] Technically, we integrate the CMF range from 10^{-4}to10 $M_{\rm sonic}$, which for typical parameters corresponds to $\sim 10^{-3}$to100 $M_\odot$, but we stress that so long as we include the 'peak' of the CMF/IMF, this choice makes little difference except in the normalization of $\xi_{\rm 2d}$. To project, we also assume the average abundance $n_0(z)$ is flat out to $\pm 2\,h$, but changing this limit or assuming an exponential $n_0 \propto \exp\,(-z/h)$ has only weak effects.

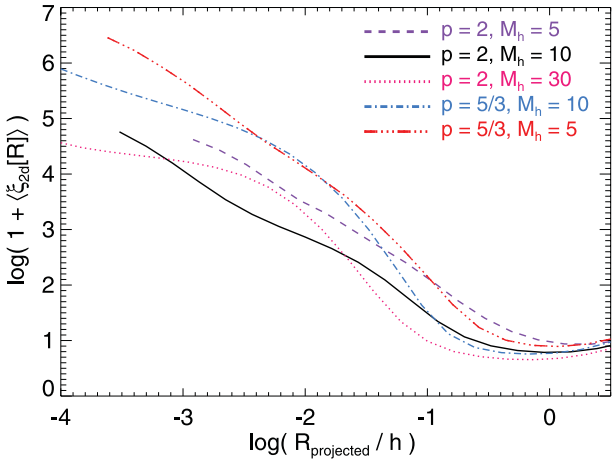

Figure 2. The (exact) predicted two-dimensional correlation function between cores of all masses – this should be comparable to the observed (projected) star–star correlation function (averaged over the IMF range of stellar masses). The predictions are qualitatively similar in all cases, but complicated second-order differences arise. Models with turbulent spectral index $p = 5/3$ are similar to those with $p = 2$ but a higher $\mathcal{M}_h$ by a factor of $\sim$2, $\mathcal{M}(r) \propto r^{(p-1)/2}$ falls off more slowly at the small scales of interest. At fixed p, lower values of $\mathcal{M}_h$ produce slightly steeper, more power-law-like behaviour. The more pronounced flattening of ξ on small scales with higher $\mathcal{M}_h$ arises because the line-of-sight integral is dominated by the (larger) power near large scales.

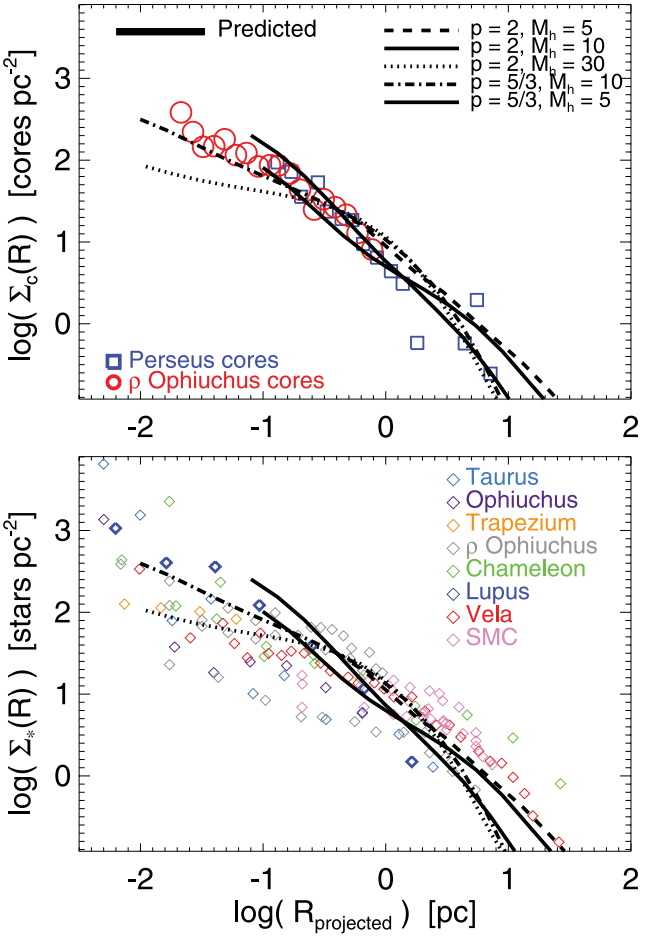

Figure 3. Mean surface density $\Sigma_*(R)$ of stars around a random star: this is proportional, by definition, to $1 + \langle \xi_{2d}(R) \rangle$ in Fig. 2. We compare the model predictions (line styles are the same as in Fig. 2; normalized by the mean surface density of the observed systems and scale height $h = 200$ pc) to observations of the corresponding core–core cross-correlation (top; points from Stanke et al. 2006; Enoch et al. 2008) and a compilation of observations of the star–star cross-correlation (bottom; points from Simon 1997; Nakajima et al. 1998; Hartmann 2002; Hennekemper et al. 2008; Kraus & Hillenbrand 2008). The agreement is reasonably good over the dynamic range observed, and the observational scatter in the shape of ξ_{2d} is similar to that predicted in Fig. 2. The models do not extend to the sharp rise in stellar clustering at scales $\lesssim$0.01 pc, usually attributed to binaries.

In Fig. 3, we compare the projected ξ_{2d} to a compilation of observations of both the star–star and core–core autocorrelation functions. Typically, the observations are plotted not as ξ_{2d} but as Σ_*, defined as the average surface number density $dN/dA(R_p)$ of companions at a radius R_p from the primary. By definition, this is trivially related to ξ_{2d} as

$$\Sigma_*(R_p) = \langle \Sigma_* \rangle (1 + \xi_{2d}). \quad (33)$$

Here, $\langle \Sigma_* \rangle$ is undetermined – it depends both on the absolute background galaxy properties which set the scale of the problem (h, ρ_0, etc.) and on the uncertain star formation efficiencies (fraction of gas which will actually turn into stars). We treat it as arbitrary and simply compare the profile shape. We normalize R to an absolute physical scale by assuming an MW-like scale height $h = 200$ pc for the gas.

We can gain some (approximate) insight into the functional form of ξ_{2d} on small scales from equation (28). Assume $r \ll h$ (the dynamic range of most interest), in the limit of equation (29), so $\mathcal{M}^2(r) \ll \mathcal{M}_h^2$ as well, and expand to leading order in $\mathcal{O}(r/h)$ and $\mathcal{O}(\mathcal{M}_h^{-1})$ (series expanding equation 13 around $S = S_0$); finally, make the simple approximation that projection to ξ_{2d} multiplies $\xi(r)$ by one power of R and that we can treat the mass averaging as a normalization correction. After some tedious algebra, we obtain

$$1 + \xi_{2d} \propto \frac{\left(1 + \frac{3}{8}\, x^{p-1}\right)^{1/4}}{x^{(p-1)/2-1}} \left[\frac{\mathcal{M}_h^{-2+\frac{4}{(p-1)}}}{\sqrt{2}} \frac{(1 + x^{p-1})}{x^2} \right]^{\frac{1}{p-1}+\epsilon} \quad (34)$$

$$\propto \frac{(1+x)\left(1 + \frac{3}{8}\, x\right)^{1/4}}{x^{3/2}} + \mathcal{O}(\ln^{-1} \mathcal{M}_h) \qquad (p = 2), \quad (35)$$

where $x \equiv R/R_{\rm sonic}$ and $\epsilon = \ln\left[x^{-2}\,(1 + x^{p-1})\right]/4 \ln(\mathcal{M}_h)$. Although we have made a number of simplifications, we recover all the key behaviours in Fig. 2: the predicted $\xi_{2d}(R)$ is an approximate power law [because $\rho_{\rm crit}(r)$ is so], which scales steeply [$\propto R^{-(1.5-2.3)}$ for $p = 5/3$–2] on small scales, then flattens around the sonic length [first to $\propto R^{-(0.5-1.0)}$ and then $R^{-0.25}$]. The 'steepening' below $R_{\rm sonic}$ is caused by the steeper dependence of $\rho_{\rm crit}$ on R at these scales (thermal support preventing collapse); the gradual run at larger scales from the logarithmic run in S with $\mathcal{M}(r)$.

Although it is less precisely defined, we can also make some estimate of the fraction of stars formed in an 'isolated' (non-clustered) mode. Specifically, in analogy to our derivation of equation (24), we begin with the probability that a core (last-crossing event) at $f_\ell(S[M])$ is embedded in a larger region $S_0[r]$ with some $\delta_0(S_0)$; we can then calculate the probability that this region contains zero additional last-crossing events. This latter probability is just given by $1 - \int_{S_0}^{S_i} dS'\, f_\ell(S' \mid \delta_0)$ from equation (2), i.e. one minus the total probability of a crossing at $S > S_0$. After some algebra, we obtain the probability of a core of mass M having no additional crossings

within the parent radius $r[S]$:

$$f_{\rm iso}(<r\,|\,M) = 1 - \int_{-\infty}^{\infty} {\rm d}\delta_0 \int_{S_0}^{S_i} {\rm d}S' \, \frac{f_\ell(S\,|\,\delta_0)}{f_\ell(S)} \, f_\ell(S'\,|\,\delta_0) \, P_0(\delta_0\,|\,S_0[r]). \quad (36)$$

If we take the limits ${\rm d}B/{\rm d}S \gg B/S \gg 1$, we can obtain the approximate scaling $f_{\rm iso}(r<r_1\,|\,M[r_0]) \sim \ln^{-1}(r_1/r_0)\,(r_1/r_0)^{-{\rm d}B/{\rm d}S}$. In greater detail, if we solve this for a linear barrier and assume the less restrictive ${\rm d}B/{\rm d}S \gtrsim 1$ and $r \ll h$, and insert $B(r)$ and $S(r)$ defined above, we finally obtain

$$f_{\rm iso}(<r\,|\,S) \approx \frac{2}{3}\left|\frac{{\rm d}B}{{\rm d}S}\right|^{-1} P_0(B[S]-B[S_0]\,|\,S-S_0[r]) \quad (37)$$

$$\sim 0.15\left[\ln\left(1+\frac{r}{R_{\rm sonic}}\right)\right]^{-1/2}\left(\frac{r}{R_{\rm sonic}}\right)^{-0.65}, \quad (38)$$

where in the latter we insert $p=2$ and $\mathcal{M}_h \sim 5$–30 (the result is very weakly dependent on $\mathcal{M}_h$). This should translate to the fraction of cores formed without a companion core inside of r. We caution that if only a small fraction of cores make stars, the fraction of stars formed without another star inside $<r$ will be higher. Moreover, if cores produce multiple stars (recall that we do not explicitly treat binaries here), the fraction of isolated stars will be even lower. Regardless of these uncertainties, we see that the absolute number of cores/stars formed without neighbours inside a radius r is small even for r near the sonic length, and falls rapidly as we expand the 'search radius'.

6 DISCUSSION

We have developed an analytic theory for the clustering properties of protostellar cores in a supersonically turbulent density field. In Paper I, we developed an excursion-set theory for lognormal density fluctuations in the ISM, and applied it to the mass functions and clustering of GMCs – the 'first-crossing distribution' (distribution of bound masses on the largest self-gravitating scales). In Paper II, we showed that this could be extended to predict the protostellar core MF by defining the 'last-crossing distribution' (distribution of masses on the *smallest* scales on which they are self-gravitating and non-fragmenting). Here, we extend this method to define the conditional last-crossing mass function, as a function of density on larger scales: i.e. the 'two-barrier last-crossing problem'. We use this to analytically derive the correlation function of these cores as a function of separation (and core mass), on all scales from the core itself to galactic scales. This should directly translate to the correlation properties of newly formed stars, independent of the mass conversion/star formation efficiency.

We find that, on *large* scales $\gtrsim h$ (the disc scale height), cores are weakly biased. Core formation, therefore, is less sensitive to galaxy-scale overdensities, except insofar as those overdensities collect/drive the dense gas. This is related to our derivation in Paper I of the clustering of GMCs: they themselves are not strongly biased (relative to the rest of the dense gas) on large scales, provided there is sufficient gas present and cooling is efficient. Moreover, we caution that on scales $\gtrsim h$, global modes such as spiral waves may be important, and we cannot assume that quantities like Σ or Ω are constant. Therefore, the relation to e.g. the global Schmidt–Kennicutt law and observations of star formation efficiency versus galaxy structure (e.g. Leroy et al. 2008; Foyle et al. 2010) is only approximate.

On scales $\ll h$, however, cores cluster very strongly. The formal three-dimensional clustering amplitudes at small scales are enormous – in other words, stars form in a clustered manner. The approximate conditional mass function (on small scales) in equation (19) illustrates why. On small scales, the 'run' in $S(R)$ given by equation (13) (hence $\Delta S \equiv S - S_0$ in equation 19) is small because $\mathcal{M}^2(R)$ is small. As this vanishes, the P_0 term in equation (19) becomes extremely sharply peaked around $\rho(R_0) = \rho_{\rm crit}(R)$ – so the CMF/IMF-averaged conditional mass function approaches a step function in $\rho(R_0)$ on some larger scale. Given the same arguments, the fraction of stars formed in an 'isolated' mode should scale as $\mathcal{O}({\rm d}B/{\rm d}S)^{-1}$; near the sonic length, this is approximately $|{\rm d}B/{\rm d}S|^{-1}_{R=R_{\rm sonic}} \lesssim 0.1$.

Physically, the meaning of this is as follows: as we average on smaller scales approaching the sonic length, the local rms Mach numbers decline rapidly ($\mathcal{M}^2 \propto r^{p-1}$), so the contribution to density fluctuations [the variance $S(R)$, which is directly tied to the Mach number in supersonic turbulence] also drops. Moreover, the threshold density for collapse continues to rise. Therefore, the smallest scale at which a region is going to be self-gravitating (or avoid fragmentation) is essentially 'imprinted' by the density by fluctuations driven on larger scales. It is unlikely to 'wander' much across the barrier on smaller scales since fluctuations are small.

As a result, stars preferentially form in larger scale overdense regions which must themselves (on some scale) be self-gravitating. The characteristic scale of the 'parent' systems – i.e. the characteristic scale at which the clustering amplitude will fall off, is the scale where $S(R)$ begins to run significantly with R. Moreover, this is by definition the characteristic scale of the *first-crossing* distribution, which we identified in Paper I with GMCs, and showed there has a characteristic scale of $\sim h$ – just set by the global turbulent Jeans length. In short, stars form inside of GMCs, in strongly clustered fashion, with the characteristic length of that clustering set by $\sim h$.

These arguments are quite general: the fundamental statement is that, since most of the power in the turbulent velocity field is on large scales ($\sim h$), star formation must be strongly clustered below that scale. This is true for any plausible turbulent power spectrum. We show explicitly that a qualitatively similar scaling results for turbulent spectral indices $p \sim 5/3$–2, and large-scale Mach numbers $\mathcal{M}_h \sim 5$–30. However, the details of the correlation function do depend on these values, in a non-trivial manner. For example, the slope on small scales $\xi_{\rm 2d} \propto R_p^{-\alpha}$ is an approximate power law with values $\alpha \approx 0.5$–1.0; it can flatten significantly to $\alpha \approx 0.1$–0.5 on sufficiently small scales if the Mach numbers are sufficiently large.[4]

We compare the predicted correlation functions to observations of both protostellar cores and young stars, and find that they agree well on the applicable scales. The scatter in the shape of observed

[4] If power were not concentrated on large scales, for example if the variance S rose steeply and continuously down to small scales, then at almost all scales around a core/star we would have $S_0 \ll S$ in equation (28), hence predict $1+\xi \approx 1 + (B^2/S)\,(S_0/S) = 1 + \nu^2\,(S_0/S)$, where ν represents the number of standard deviations needed for a core to form. Thus, if cores can 'easily' form near the mean density ($\nu \lesssim 1$), and/or the power in the density field continued to rise down to small scales ($S_0 \ll S$), $\xi \ll 1$ and $\Sigma_*(R_p) = \langle\Sigma_*\rangle(1+\xi) \approx \langle\Sigma_*\rangle$ would be nearly flat as a function of radius, in stark disagreement with the observed clustering. For example, for $p=1.1$ and a Toomre $Q=0.01$, $\Sigma_*(R_p)$ in Fig. 3 increases by a factor of <2 from $R=500$ to 0.01 pc.

correlation functions is also intriguingly similar to the range predicted from the parameter variations above.[5]

On the smallest scales $\ll 0.1$ pc, our prediction does not rise as steeply as the observed stellar correlation functions. This is expected, since this effect comes primarily from binary and multiple stellar systems, which we do not explicitly predict since the fragmentation events are on a subcore scale. Our derivation implicitly samples a 'snapshot' within fully developed turbulence. We would need to treat cores collapsing in time to follow successive fragmentation and/or stellar accretion as the cores contract and form stars, but this will in turn depend in detail on the gas thermodynamics and stellar feedback (see e.g. Krumholz et al. 2009; Peters et al. 2010). In Paper II, we discuss in detail how this (and other time-dependent processes) may modify the relation between CMF and IMF; if the effect on the density distribution and/or multiplicity is truly scale-free, these effects factor out in our analysis here, but there is no strong reason to believe it would be so. However, on larger scales, theoretical arguments (and some observations) suggest that the primary role of feedback is to regulate the turbulent cascade and generate outflows, as well as to regulate the core-to-stellar mass conversion efficiencies (see e.g. Matzner & McKee 2000; Mac Low & Klessen 2004; Alves, Lombardi & Lada 2007; Enoch et al. 2008; Veltchev, Klessen & Clark 2011); in that regime, our conclusions should be robust. Improving the predictions here by taking these processes into account may be possible in the time-dependent formulation of the excursion-set ISM model developed in Paper I, since that could follow the simultaneous growth of fluctuations and collapse of a given subregion, coupled to appropriate models for the thermodynamics and stellar feedback.

ACKNOWLEDGMENTS

We thank Chris McKee and Eliot Quataert for helpful discussions in the development of this work, as well as Eli Bressert, Stella Offner and our referee, Federico Pelupessy, for a number of suggestions and comments. Support for PFH was provided by NASA through Einstein Postdoctoral Fellowship Award Number PF1-120083 issued by the Chandra X-ray Observatory Center, which is operated by the Smithsonian Astrophysical Observatory for and on behalf of the NASA under contract NAS8-03060.

[5] It does appear that in some systems, the stellar correlation function may be slightly flatter on small scales than the core correlation function, but this will inevitably occur in time as stars move from their birthplace, and so it is difficult to disentangle without knowing the velocity and age distributions of the stars.

REFERENCES

Alves J., Lombardi M., Lada C. J., 2007, A&A, 462, L17
Bate M. R., Clarke C. J., McCaughrean M. J., 1998, MNRAS, 297, 1163
Bressert E. et al., 2010, MNRAS, 409, L54
Clarke C. J., Bonnell I. A., Hillenbrand L. A., 2000, in Mannings V., Boss A. P., Russell S. S., eds, Protostars and Planets IV. Univ. Arizona Press, Tucson, p. 151
de Wit W. J., Testi L., Palla F., Zinnecker H., 2005, A&A, 437, 247
Enoch M. L., Evans N. J. II, Sargent A. I., Glenn J., Rosolowsky E., Myers P., 2008, ApJ, 684, 1240
Foyle K., Rix H.-W., Walter F., Leroy A. K., 2010, ApJ, 725, 534
Gies D. R., 1987, ApJS, 64, 545
Gomez M., Hartmann L., Kenyon S. J., Hewett R., 1993, AJ, 105, 1927
Hansen C. E., Klein R. I., McKee C. F., Fisher R. T., 2012, ApJ, 747, 22
Hartmann L., 2002, ApJ, 578, 914
Hennebelle P., Chabrier G., 2008, ApJ, 684, 395
Hennekemper E., Gouliermis D. A., Henning T., Brandner W., Dolphin A. E., 2008, ApJ, 672, 914
Hopkins P. F., 2012a, MNRAS, 423, 2016 (Paper I)
Hopkins P. F., 2012b, MNRAS, 423, 2037 (Paper II)
Hopkins P. F., 2012c, MNRAS, preprint (arXiv:1204.2835)
Klessen R. S., Burkert A., 2000, ApJS, 128, 287
Kraus A. L., Hillenbrand L. A., 2008, ApJ, 686, L111
Krumholz M. R., Klein R. I., McKee C. F., Offner S. S. R., Cunningham A. J., 2009, Sci, 323, 754
Lada C. J., Lada E. A., 2003, ARA&A, 41, 57
Larson R. B., 1994, in Clemens D. P., Barvainis R., eds, ASP Conf. Ser. Vol. 65, Clouds, Cores, and Low Mass Stars. Astron. Soc. Pac., San Francisco, p. 125
Leroy A. K., Walter F., Brinks E., Bigiel F., de Blok W. J. G., Madore B., Thornley M. D., 2008, AJ, 136, 2782
Mac Low M.-M., Klessen R. S., 2004, Rev. Modern Phys., 76, 125
Matzner C. D., McKee C. F., 2000, ApJ, 545, 364
Mo H. J., White S. D. M., 1996, MNRAS, 282, 347
Nakajima Y., Tachihara K., Hanawa T., Nakano M., 1998, ApJ, 497, 721
Oey M. S., King N. L., Parker J. W., 2004, AJ, 127, 1632
Ostriker E. C., Gammie C. F., Stone J. M., 1999, ApJ, 513, 259
Padoan P., Nordlund A., Jones B. J. T., 1997, MNRAS, 288, 145
Parker R. J., Goodwin S. P., 2007, MNRAS, 380, 1271
Peters T., Klessen R. S., Mac Low M.-M., Banerjee R., 2010, ApJ, 725, 134
Portegies Zwart S. F., McMillan S. L. W., Gieles M., 2010, ARA&A, 48, 431
Schilbach E., Röser S., 2008, A&A, 489, 105
Simon M., 1997, ApJ, 482, L81
Stanke T., Smith M. D., Gredel R., Khanzadyan T., 2006, A&A, 447, 609
Vazquez-Semadeni E., 1994, ApJ, 423, 681
Veltchev T. V., Klessen R. S., Clark P. C., 2011, MNRAS, 411, 301
Zhang J., Hui L., 2006, ApJ, 641, 641
Zhang Q., Fall S. M., Whitmore B. C., 2001, ApJ, 561, 727

This paper has been typeset from a TEX/LATEX file prepared by the author.